[3]Hollkamp, J. J., "Multimodal Passive Vibration Suppression with Piezoelectrics," AIAA Paper 93-1683, 1993.

[4]Hollkamp, J. J., and Starchville, T. F., "A Self-Tuning Piezoelectric Vibration Absorber," *Journal of Intelligent Materials Systems and Structures*, Vol. 5, No. 4, 1994, pp. 559–566.

[5]Rew, K.-H., Han, J. H., and Lee, I., "Adaptive Multimodal Vibration Control of Winglike Composite Structure Using Adaptive Positive Position Feedback," AIAA Paper 2000-1422, 2000.

Level Flight Trim and Stability Analysis Using Extended Bifurcation and Continuation Procedure

N. Ananthkrishnan* and Nandan K. Sinha†
Indian Institute of Technology, Bombay 400 076, India

I. Introduction

AIRCRAFT that are designed for rapid maneuvering and for controlled flight at high angles of attack often experience a variety of flight instabilities, that result in nonlinear phenomena, such as wing rock and spin, or in loss-of-control problems, such as yaw departure. The bifurcation and continuation method is the standard tool in use today for the analysis and prediction of flight instability phenomena. The standard bifurcation analysis (SBA) procedure can be used to study any dynamic system of the following form:

$$\dot{\boldsymbol{x}} = \boldsymbol{f}(\boldsymbol{x}, u, \boldsymbol{p}) \tag{1}$$

where $\boldsymbol{x}$ is the vector of state variables, u is the control parameter being varied, and $\boldsymbol{p}$ is the vector of parameters kept fixed. The equations for rigid aircraft flight dynamics (see the Appendix) appear as a set of eight first-order differential equations of precisely the form of Eq. (1), with a typical choice of states, control parameter, and fixed parameters, as follows:

$$\boldsymbol{x} = [M, \alpha, \beta, p, q, r, \phi, \theta], \qquad u = \delta e, \qquad \boldsymbol{p} = [\eta, \delta a, \delta r]$$

where M is the Mach number, η is the throttle as a fraction of maximum thrust, and the other variables have their standard meanings. Thus, the SBA procedure can be directly applied to the aircraft flight dynamic equations in the Appendix. When a starting trim condition $(\boldsymbol{x}_0, u_0, \boldsymbol{p}_0)$ is given, the SBA procedure uses a continuation algorithm to compute the entire branch of trim states $\boldsymbol{x}$ with varying values of the control u, but with $\boldsymbol{p}_0$ held fixed. The continuation algorithm also calculates the Jacobian matrix of the dynamic system Eq. (1) at each trim, which is used to indicate the stability of that trim. Bifurcation points along the trim branch can be located, and bifurcating solution branches such as limit cycles can be tracked by the SBA procedure. The SBA procedure has been employed in this manner to study the onset of flight instabilities such as wing rock, spiral divergence, and spin and also to devise recovery strategies from difficult flight conditions such as spin, to prevent undesirable phenomena such as jump in roll maneuvers, and as an aid to control law design.[1–4] A detailed introduction to the SBA procedure has been provided by Goman et al.[5]

The different trims along a branch computed by the SBA procedure do not, in general, share a common value of a state variable such as angle of attack or Mach number. For example, when the SBA procedure is started with a level flight trim and the elevator is used as the control, it is seen that other computed trims along the branch do not correspond to level flight. However, there are several reasons for desiring the bifurcation analysis procedure to be able to constrain one or more states to their values at the starting point. A bifurcation analysis procedure that can account for state variable constraints could be used to evaluate aircraft performance parameters such as the maximum roll rate in zero-sideslip roll maneuvers, or the maximum turn rate in a level turn. The ability to generate successive trim states, all satisfying a common level flight condition, would be a useful input to control law design. Also, a bifurcation analysis that can handle state constraints may be expected to show results that correlate better with flight tests because it can be used to reproduce maneuvers flown by pilots. A constrained bifurcation analysis (CBA) procedure was first used by Ananthkrishnan and Sudhakar[6] to study roll maneuvers with a zero-sideslip constraint, followed by a study of velocity vector roll maneuvers by Modi and Ananthkrishnan.[7] The CBA procedure and its application to level flight maneuvers has been described in a recent paper by Pashilkar and Pradeep.[8] The CBA procedure requires the constraint equations to be appended to the equations for the aircraft dynamics, giving an augmented set of state plus constraint equations, as follows:

$$\dot{\boldsymbol{x}} = \boldsymbol{f}(\boldsymbol{x}, u, \boldsymbol{p}), \qquad \boldsymbol{y} = \boldsymbol{g}(\boldsymbol{x}) = 0 \tag{2}$$

where $\boldsymbol{g}$ is an m-dimensional vector function that represents the constraints. Let $\boldsymbol{x}$ have dimension n. Then, to use a continuation algorithm with the set of $(n + m)$ equations in Eq. (2), it is necessary to have $(n + m + 1)$ variables or unknowns. Clearly, the additional m variables must be obtained from the parameter vector $\boldsymbol{p}$. Therefore, as many elements of $\boldsymbol{p}$ are freed as there are constraint equations in the augmented set, so that the CBA problem is well posed. A continuation algorithm is then used to compute the trim states along with the values of the freed parameters as a function of the control u. All such computed trims naturally satisfy the imposed constraint, and the computed values of the freed parameters indicate how they should be varied in practice with the control u, to achieve the demanded constraints.

However, the CBA procedure is unsatisfactory in two respects. First, the CBA procedure with the augmented set of equations in Eq. (2) does not provide correct information about the stability of the trim points. This is because present continuation algorithms internally compute the Jacobian of the augmented set of equations, where they regard the constraint equations at par with the state equations. The eigenvalues computed from the augmented Jacobian matrix do not correctly reflect the stability of the constrained trim state. This may be regarded more as a limitation of the continuation software than a shortcoming of the CBA procedure. However, previous attempts to overcome this problem required either numerical simulations or extraction and separate computation of the appropriate submatrix of the Jacobian matrix at each trim point, both procedures being tedious and inefficient. Second, as part of the CBA procedure, it is of interest to identify possible departures from the constrained flight condition, which may be expected when the constrained trim states lose stability. The CBA procedure, however, cannot compute solutions that depart from the constraints because the analysis always includes the constraint equations. Informally speaking, in the CBA procedure, the constraints are always on, hence, only trims that obey the constraints are computed. Thus, previous attempts at carrying out bifurcation analysis in the presence of constraints have been hampered by the inability of the CBA procedure to extract stability information from the continuation algorithm and its inability to trace departures from the constrained trim states.

In this Note, we propose a new method called the extended bifurcation and continuation procedure that overcomes these drawbacks of the CBA procedure. The extended bifurcation analysis (EBA) procedure, in the presence of state variable constraints, computes trim points satisfying the constraints along with their correct stability and tracks departures from the constrained flight at points where the trim states lose stability. Thus, it becomes possible to generate complete bifurcation diagrams for the aircraft dynamics in constrained flight maneuvers using the EBA procedure. In the rest of

Received 10 May 2000; revision received 3 January 2001; accepted for publication 5 June 2001.

*Assistant Professor, Department of Aerospace Engineering; akn@aero.iitb.ac.in; currently Visiting Assistant Professor of Aeronautics, California Institute of Technology, Pasadena, CA 91125; akn@caltech.edu. Member AIAA.

†Ph.D. Student, Department of Aerospace Engineering; nandan@aero.iitb.ac.in.

this Note, the choice of the elements of the vector $\boldsymbol{p}$ to be freed for a given set of constraints is discussed briefly, following which the new EBA procedure is described. The EBA procedure is illustrated for two common cases of constrained flight: straight and level flight and zero sideslip level turn. The utility of the EBA method is underlined by displaying results in the form of standard aircraft performance and stability plots, such as that of thrust required for straight and level flight vs the Mach number, or the familiar longitudinal trim chart of angle of attack vs elevator deflection.

II. Discussion of Constraints

In any constrained bifurcation problem, when the vector $\boldsymbol{p}$ contains fewer parameters than the number of constraints $\boldsymbol{g}$ in Eq. (2), then the constraints are untenable. However, for a well-formulated problem with m independent constraints, $\boldsymbol{p}$ will normally contain m or more parameters. In case there are more parameters than constraints, one is inevitably led to the question of which parameters should be freed to satisfy the given set of constraints. To answer this question, differentiate each constraint equation $g_i(\boldsymbol{x}) = 0$ with respect to time, as follows, to see how $\boldsymbol{p}$ enters the constraint equations:

$$\dot{y}_i = \frac{\partial g_i}{\partial x_j}\dot{x}_j = \frac{\partial g_i}{\partial x_j} f_j(\boldsymbol{x}, u, \boldsymbol{p}) = 0 \tag{3}$$

Thus, an element of $\boldsymbol{p}$ can influence the ith constraint provided the corresponding coefficient $\partial g_i/\partial x_j$ is nonzero. This coefficient can be thought of as a weighting that quantifies the effect of the particular parameter on the constraint. Incidentally, the CBA problem as posed earlier can be viewed as a regulation problem in the language of control theory, where $\boldsymbol{y}$ are the outputs to be regulated to zero and the derivative in Eq. (3) is simply the Lie derivative $\mathcal{L}_f(g_i)$. Then the question of the influence of a particular parameter on the ith output y_i can be answered in terms of the relative degree of the output with respect to that parameter. Instead, it is instructive as well as economical to consider a couple of examples of constraints of relevance to aircraft flight in an attempt to resolve this matter. In both the examples that follow, the control parameter u is the elevator deflection.

A. Example Constraint 1

Consider a constraint equation $y = g(\boldsymbol{x}) = M - M_0 = 0$, where the Mach number is desired to be held constant at a value M_0. When y is differentiated with time, as in Eq. (3), and the first of Eqs. (A1) is used, the constraint equation appears as

$$\dot{y} = \dot{M} = (1/mv_s)\left[T_m \eta \cos\alpha \cos\beta - \tfrac{1}{2} C_D \rho (v_s M)^2 S - mg \sin\gamma\right] = 0$$

The only element of $\boldsymbol{p}$ that appears on the right-hand side is the throttle parameter η, which is intuitively the obvious choice of control to hold the Mach number fixed.

B. Example Constraint 2

Consider a constraint equation $y = g(\boldsymbol{x}) = \phi = 0$, which corresponds to a wings level constraint. Along similar lines as, for example, constraint 1, and using the first of Eq. (A3), it is possible to write

$$\dot{y} = \dot{\phi} = p + q \sin\phi \tan\theta + r \cos\phi \tan\theta = 0$$

where the parameter $\boldsymbol{p}$ does not appear at all. In this case, it is necessary to differentiate once over to obtain

$$\ddot{y} = \ddot{\phi} = \dot{p} + \dot{q} \sin\phi \tan\theta + \dot{r} \cos\phi \tan\theta + [\text{other terms without } \boldsymbol{p}] = 0$$

When substitution is made for $\dot{p}$, $\dot{q}$, and $\dot{r}$ from Eq. (A2), the right-hand side of the preceding equation can be seen to contain both the aileron and rudder deflections. Thus, in principle, either aileron or rudder may be used to satisfy the wings level constraint. In practice, it is usually the aileron that is used, though there are instances of aircraft that, especially at high angles of attack, may lose aileron effectiveness and may need to use the rudder for roll control. In fact, the CBA procedure actually provides an elegant way to locate flight regimes where control effectiveness is lost. In such flight regimes, the CBA procedure will show markedly larger values of the corresponding freed parameter, perhaps even exceeding its physical limits. This is especially useful when dealing with large amounts of nonlinear aerodynamic data. The SBA procedure, in contrast, with fixed parameter $\boldsymbol{p}$, is not capable of being used in this manner.

III. EBA

The key to the EBA procedure is to recognize that the constraint equations in Eq. (2) are relevant only insofar as they establish the variation of the freed parameters (as a function of the control parameter) required to satisfy the constraints. They have no role to play in determining the stability of the constrained trim states, which is decided solely by the dynamic equations for the state variables. The EBA procedure, therefore, divides the CBA problem into two separate steps, as follows:

Step 1 is the determination of parameter schedules. In this step, the augmented set consisting of the dynamic equations for the states plus the constraint equations, as in Eq. (2), are considered, and a CBA procedure is carried out with varying control u. However, the results are used only to determine the variation of the freed parameters as a function of the control u. Thus, the parameter schedules required to satisfy the constraints are known at the end of the first step.

Step 2 is the determination of stability and departures. Let the parameter schedules computed by the CBA procedure in the first step be denoted by $\boldsymbol{p}_1(u)$, the corresponding trim states by $\boldsymbol{x}_c(u)$, and the vector of parameters not freed by $\boldsymbol{p}_2$. In the second step, only the dynamic equations for the state variables are considered, as follows:

$$\dot{\boldsymbol{x}} = \boldsymbol{f}(\boldsymbol{x}, u, \boldsymbol{p}_1(u), \boldsymbol{p}_2) \tag{4}$$

and an SBA procedure is carried out with varying u and $\boldsymbol{p}_1$ varying with u according to the parameter schedules $\boldsymbol{p}_1(u)$ computed in step 1. The parameter vector $\boldsymbol{p}_2$ is held fixed. Note that the SBA procedure now computes all trims with the parameter schedule $\boldsymbol{p}_1(u)$. Among these are the constrained trim states $\boldsymbol{x}_c(u)$ computed in step 1. The correct stability of these trims is also calculated by the SBA procedure, now that the parameters $\boldsymbol{p}_1$ appear only as functions of the control u and, hence, do not enter in the Jacobian matrix for the function $\boldsymbol{f}$ in Eq. (4). In addition, the trims computed by the SBA procedure for Eq. (4) could also include other solutions, different from the constrained trim states $\boldsymbol{x}_c(u)$, for the same parameter schedules $\boldsymbol{p}_1(u)$. These solutions either represent departures from the constrained trim states at points of instability, or other unconnected trim branches. The new EBA procedure, thus, manages to overcome both the drawbacks of the existing CBA procedure and can compute constrained trims, stability, and departures from the prescribed constrained flight. The EBA procedure can be implemented as a first step CBA procedure followed by a second step SBA procedure using any standard continuation algorithm.

The capabilities of the EBA procedure are now illustrated by applying it to two different constrained flight maneuvers, using the publicly available AUTO continuation software.[9] Aircraft data for the computations have been taken from Ref. 10.

A. Straight and Level Flight

The straight and level flight constraint is the standard trim condition for the evaluation of flight stability and for the design of control laws and requires the aircraft to fly along a straight-line path at a fixed altitude with zero sideslip and wings level. The augmented equation set for this flight maneuver consists of the following 11 equations (8 state equations, as in the Appendix, and 3 constraint equations):

$$\dot{\boldsymbol{x}} = \boldsymbol{f}(\boldsymbol{x}, u, \boldsymbol{p}), \qquad \gamma = 0, \qquad \beta = 0, \qquad \phi = 0 \tag{5}$$

with $\boldsymbol{x} = [M, \alpha, \beta, p, q, r, \phi, \theta]$, $u = \delta e$, and $\boldsymbol{p} = [\eta, \delta a, \delta r]$. It can be easily verified, along the lines of the constraint examples in the preceding section, that the three parameters in the vector $\boldsymbol{p}$ do influence the three constraints in Eq. (5). Thus, in step 1 of the EBA procedure, a CBA of the augmented system in Eq. (5) is carried out with all three parameters (throttle, aileron, and rudder) freed, resulting in a set of 11 variables (8 states and 3 freed parameters)

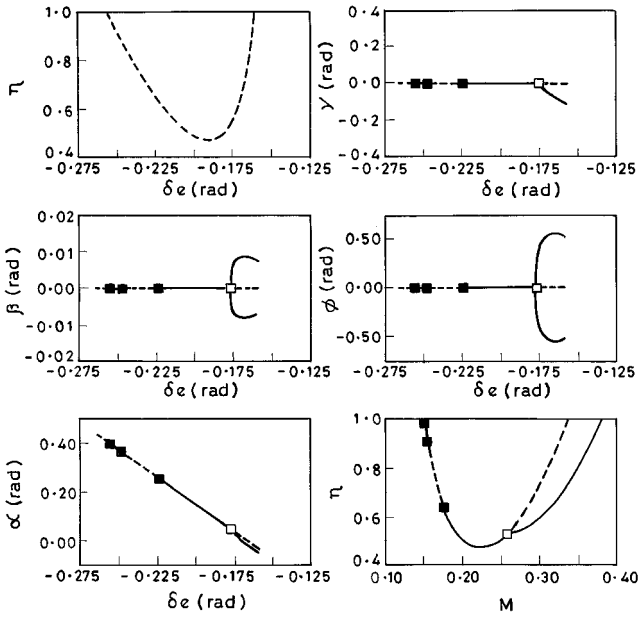

Fig. 1 Straight and level flight: (top left) variation of throttle parameter η with elevator deflection δe and (others) various bifurcation diagrams (full line, stable trim; dashed line, unstable trim; filled square, Hopf bifurcation; and empty square, pitchfork bifurcation).

plus a control parameter u, which is the elevator deflection. A starting straight and level flight trim point, required by any continuation algorithm, is obtained from elsewhere and provided as follows:

$$\boldsymbol{x}: [M = 0.2, \alpha = 10.68 \text{ deg}, \ \beta = 0, p = 0, q = 0,$$

$$r = 0, \phi = 0, \theta = 10.68 \text{ deg}]$$

$$u: \delta e = -12 \text{ deg}$$

$$\boldsymbol{p}: [\eta = 0.523, \delta a = 0, \delta r = 0]$$

All other straight and level flight trims are then computed using AUTO with varying elevator deflection. Computations are stopped at the upper limit of the throttle, $\eta = 1$. From this computation, the variation of the throttle, aileron, and rudder required to maintain straight and level flight, is obtained as a function of elevator deflection. The variation of the throttle η, which represents the thrust required to maintain level flight, is plotted in Fig. 1 for varying values of the elevator deflection. The plot has a standard parabolic shape associated with a quadratic drag polar; however, all trims are marked unstable because the CBA procedure in step 1 cannot correctly identify the stability of the constrained trims. The computed aileron and rudder deflections turn out to be identically zero, as may be expected, and are, therefore, not plotted here. Also, plots for variation of the state variables as a function of the elevator deflection, obtained at this step, show only constrained trims with incorrect stability information and no departure solutions; therefore, no purpose is served by reproducing them at this stage.

In step 2 of the EBA procedure, the parameter schedules $\boldsymbol{p}_1(u)$ found in step 1, that is, $\eta(\delta e)$ as plotted in Fig. 1, $\delta a(\delta e) = 0$, and $\delta r(\delta e) = 0$, are used in Eq. (4), and an SBA procedure is carried out to compute bifurcation diagrams with elevator deflection as the control parameter. The bifurcation diagrams for the constrained variables, γ, β, and ϕ are shown in Fig. 1, where the constrained trim states obviously correspond to trims with zero values of all three variables. Stable and unstable trims are indicated in Fig. 1. Reading these plots in Fig. 1 from left to right, the points of instability are found to correspond to the Dutch roll mode (Hopf bifurcation), phugoid mode (Hopf bifurcation), phugoid mode again (Hopf bifurcation), and the spiral mode (pitchfork bifurcation). It is not the aim of this Note to describe these instabilities, but merely to point out that such instabilities can be successfully detected by the EBA procedure. Departure from the constrained flight is noticed at the pitchfork bifurcation where stable trim states with non-zero values of γ, β, and ϕ are created. These solutions can be identified from Fig. 1 to describe a descending (negative γ) flight. Other useful graphs that can be easily produced by the EBA procedure are the standard longitudinal trim plot of angle of attack with elevator deflection and the level flight performance plot of throttle (thrust required) vs Mach number, which are also included in Fig. 1. The ability to produce such plots that indicate trim states along with their stability, points of onset of instability, and departures from the constrained flight, is a unique feature of the EBA procedure.

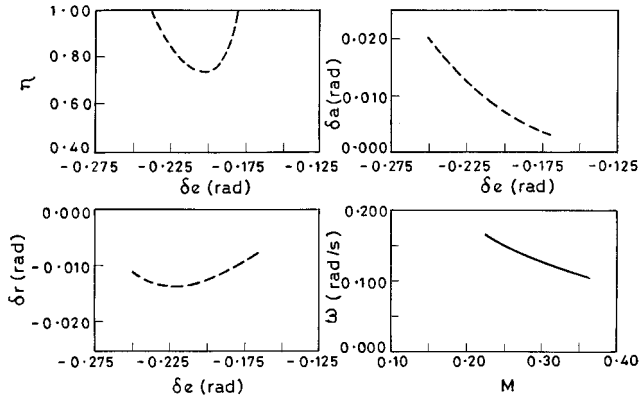

Fig. 2 Level turn: variation of throttle parameter η, aileron deflection δa, and rudder deflection δr, with elevator deflection δe, (bottom right) bifurcation diagram of the turn rate ω with Mach number M (full line, stable trim and dashed line, unstable trim).

B. Level Turns

Level turns under zero-sideslip conditions are often considered for aircraft stability and control analysis. The augmented set of equations for this constrained flight consists of the eight state equations in the Appendix plus three constraint equations:

$$\dot{\boldsymbol{x}} = \boldsymbol{f}(\boldsymbol{x}, u, \boldsymbol{p}), \qquad \gamma = 0, \qquad \beta = 0, \qquad \phi = 50 \text{ deg} \qquad (6)$$

where $\boldsymbol{x} = [M, \alpha, \beta, p, q, r, \phi, \theta]$, $u = \delta e$, $\boldsymbol{p} = [\eta, \delta a, \delta r]$, and the constraint on the roll angle has been chosen to be 50 deg, which corresponds to a load factor of 1.56. In step 1 of the EBA procedure, a CBA procedure for Eq. (6) is carried out with the elevator deflection as the control parameter u. All three parameters in $\boldsymbol{p}$ are freed, and they can be verified to influence the three constraints in Eq. (6). Computations are halted at the throttle limit of $\eta = 1$. The CBA procedure provides schedules for the parameters $\eta(\delta e)$, $\delta a(\delta e)$, and $\delta r(\delta e)$, which are shown plotted in Fig. 2. The throttle required for the turn is larger than that for straight and level flight in Fig. 1, and nonzero values of the rudder and aileron are necessary to maintain the load factor and sideslip, as could have been anticipated. In step 2 of the EBA procedure, these schedules are used in Eq. (4) to carry out an SBA procedure with the elevator deflection as the varying control u. Complete bifurcation diagrams for the level turn case are then obtained in step 2. As an example, the bifurcation diagram for the turn rate as a function of Mach number in the level turning maneuver is shown in Fig. 2. As indicated in this plot, all constrained trim states in this case are stable, and the aircraft shows no instabilities or departure tendencies.

IV. Conclusions

Previous attempts at computing aircraft trim states and their bifurcations in constrained flight maneuvers have been unsuccessful in simultaneously determining the stability of the trim states and in locating and tracking departures from the constrained flight. The reasons for the failure of the existing CBA procedure have been detailed. A new EBA procedure has been described that is able to overcome the drawbacks of the existing CBA method. The EBA procedure is used to compute trims and stability for two different level flight maneuvers, with points of instability and departure solutions being simultaneously computed. The usefulness of the EBA procedure for aircraft performance evaluation, and as an input to control law design, is evident from the results reported in this Note.

Appendix: Aircraft Dynamic Equations

The flight dynamics of rigid aircraft are described by the following set of eight first-order differential equations taken from Ref. 10:

$$\dot{M} = (1/mv_s)\left[T_m\eta\cos\alpha\cos\beta - \tfrac{1}{2}C_D(\alpha)\rho v_s^2 M^2 S - mg\sin\gamma\right]$$

$$\dot{\beta} = (1/mv_s M)\left[-T_m\eta\cos\alpha\sin\beta + \tfrac{1}{2}C_Y(\beta,\delta a,\delta r)\rho v_s^2 M^2 S + mg\sin\mu\cos\gamma\right] + (p\sin\alpha - r\cos\alpha)$$

$$\dot{\alpha} = q - (1/\cos\beta)\left\{(p\cos\alpha + r\sin\alpha)\sin\beta + (1/mv_s M)\left[T_m\eta\sin\alpha + \tfrac{1}{2}C_L(\alpha,\delta e)\rho v_s^2 M^2 S - mg\cos\mu\cos\gamma\right]\right\} \quad \text{(A1)}$$

$$\dot{p} = [(I_y - I_z)/I_x]qr + (1/2I_x)\rho(v_s M)^2 SbC_l(\alpha,\beta,p,r,\delta a,\delta r)$$

$$\dot{q} = [(I_z - I_x)/I_y]pr + (1/2I_y)\rho(v_s M)^2 ScC_m(\alpha,q,\delta e)$$

$$\dot{r} = [(I_x - I_y)/I_z]pq + (1/2I_z)\rho(v_s M)^2 SbC_n(\alpha,\beta,p,r,\delta a,\delta r) \quad \text{(A2)}$$

$$\dot{\phi} = p + q\sin\phi\tan\theta + r\cos\phi\tan\theta$$

$$\dot{\theta} = q\cos\phi - r\sin\phi \quad \text{(A3)}$$

The wind axis orientation angles μ and γ are defined as follows:

$$\sin\gamma = \cos\alpha\cos\beta\sin\theta - \sin\beta\sin\phi\cos\theta - \sin\alpha\cos\beta\cos\phi\cos\theta$$

$$\sin\mu\cos\gamma = \sin\theta\cos\alpha\sin\beta + \sin\phi\cos\theta\cos\beta - \sin\alpha\sin\beta\cos\phi\cos\theta$$

$$\cos\mu\cos\gamma = \sin\theta\sin\alpha + \cos\alpha\cos\phi\cos\theta$$

Acknowledgments

We would like to acknowledge partial support for this work by a grant from the Aeronautical Development Agency, Bangalore (India), monitored by T. G. Pai and V. S. Ranganathan; computational facilities provided by Gopal Shevare at the Associate Center for Computational Fluid Dynamics, Indian Institute of Technology, Bombay, India; and help in improving the presentation by associate editor Vivek Mukhopadhyay.

References

[1]Jahnke, C. C., and Culick, F. E. C., "Application of Bifurcation Theory to the High-Angle-of-Attack Dynamics of the F-14," *Journal of Aircraft*, Vol. 31, No. 1, 1994, pp. 26–34.

[2]Ananthkrishnan, N., and Sudhakar, K., "Prevention of Jump in Inertia-Coupled Roll Maneuvers of Aircraft," *Journal of Aircraft*, Vol. 31, No. 4, 1994, pp. 981–983.

[3]Avanzini, G., and de Matteis, G., "Bifurcation Analysis of a Highly Augmented Aircraft Model," *Journal of Guidance, Control, and Dynamics*, Vol. 20, No. 4, 1997, pp. 754–759.

[4]Littleboy, D. M., and Smith, P. R., "Using Bifurcation Methods to Aid Nonlinear Dynamic Inversion Control Law Design," *Journal of Guidance, Control, and Dynamics*, Vol. 21, No. 4, 1998, pp. 632–638.

[5]Goman, M. G., Zagaynov, G. I., and Khramtsovsky, A. V., "Application of Bifurcation Methods to Nonlinear Flight Dynamics Problems," *Progress in Aerospace Sciences*, Vol. 33, 1997, pp. 539–586.

[6]Ananthkrishnan, N., and Sudhakar, K., "Inertia-Coupled Coordinated Roll Maneuvers of Airplanes," *Journal of Aircraft*, Vol. 32, No. 4, 1995, pp. 883, 884.

[7]Modi, A., and Ananthkrishnan, N., "Multiple Attractors in Inertia-Coupled Velocity Vector Roll Maneuvers of Airplanes," *Journal of Aircraft*, Vol. 35, No. 4, 1998, pp. 659–661.

[8]Pashilkar, A. A., and Pradeep, S., "Computation of Flight Mechanics Parameters Using Continuation Techniques," *Journal of Guidance, Control, and Dynamics*, Vol. 24, No. 2, 2001, pp. 324–329.

[9]Doedel, E. J., Wang, X. J., and Fairgrieve, T. F., "AUTO94: Software for Continuation and Bifurcation Problems in Ordinary Differential Equations," Applied and Computational Mathematics Rept., California Inst. of Technology, Pasadena, CA, 1995.

[10]Fan, Y., Lutze, F. H., and Cliff, E. M., "Time-Optimal Lateral Maneuvers of an Aircraft," *Journal of Guidance, Control, and Dynamics*, Vol. 18, No. 5, 1995, pp. 1106–1112.

Near-Eigenaxis Rotation Control Law Design for Moving-to-Rest Maneuver

Hwa-Suk Oh,* Young-Deuk Yoon,† Young-Keun Chang,‡ Jai-Hyuk Hwang,§ and Sang Seok Lim¶
Hankuk Aviation University, Koyang 412-791, Republic of Korea

Introduction

IT has been widely reported that the eigenaxis rotation maneuver reduces energy consumption of spacecraft.[1–3] Bilimoria and Wie[2] showed, however, that in general the eigenaxis rotation maneuver is not time optimal. Steyn[3] presented a near-minimum-time control technique for rotating a spacecraft around its eigenaxis. The applications of the mentioned eigenaxis rotation control laws have been confined to rest-to-rest maneuvers. The immediate eigenaxis rotation is impossible when the spacecraft is initially in motion, except for the case when the angular velocity is parallel to the eigenaxis.

In this Note, a new eigenaxis rotation algorithm, which is applicable to a spacecraft initially in motion, is suggested. Even when the initial angular velocity vector is not parallel to the eigenaxis, the algorithm causes the angular velocity vector to change its direction parallel to the instantaneous eigenaxis and then induces the eigenaxis rotation. Eigenaxis rotation occurs at all phases of the maneuver except for the start phase. Thus, the suggested algorithm is referred to as a near-eigenaxis rotation control law. However, a significant improvement in energy consumption can be achieved.

Design of Attitude Control Law

Consider first a control law design procedure for a large angle maneuver. Let the spacecraft states be represented by the angular velocity vector $\boldsymbol{\omega}$ and the four-dimensional Euler parameter vector $\bar{\boldsymbol{\beta}} = [\beta_0\ \ \beta_1\ \ \beta_2\ \ \beta_3]^T$. The system kinematic equation can then be given by[4]

$$\dot{\bar{\boldsymbol{\beta}}} = \frac{1}{2}\begin{bmatrix} -\beta_1 & -\beta_2 & -\beta_3 \\ \beta_0 & -\beta_3 & \beta_2 \\ \beta_3 & \beta_0 & -\beta_1 \\ -\beta_2 & \beta_1 & \beta_0 \end{bmatrix}\boldsymbol{\omega} \equiv \frac{1}{2}G(\bar{\boldsymbol{\beta}})\boldsymbol{\omega} \quad (1)$$

The spacecraft is equipped with reaction wheels that serve as torque actuators. Dynamic equations can then be written as

$$I\dot{\boldsymbol{\omega}} = -\boldsymbol{\omega}^{\times} I\boldsymbol{\omega} - \boldsymbol{\omega}^{\times} h - u \quad (2)$$

$$\dot{h} = u \quad (3)$$

where I is the inertia matrix and h and u are the wheel angular momentum and the control torque, respectively. Among the existing methods for nonlinear control law design, one of the most powerful is Lyapunov's approach (see Refs. 5 and 6). Let the target states for a spacecraft be $\boldsymbol{\omega}_f$ and $\bar{\boldsymbol{\beta}}_f$. Then, consider a Lyapunov function given by

$$V = (\bar{\boldsymbol{\beta}} - \bar{\boldsymbol{\beta}}_f)^T(\bar{\boldsymbol{\beta}} - \bar{\boldsymbol{\beta}}_f) + \tfrac{1}{2}k_2^{-1}(\boldsymbol{\omega} - \boldsymbol{\omega}_f)^T(\boldsymbol{\omega} - \boldsymbol{\omega}_f) \quad (4)$$

Received 7 December 2000; revision received 29 March 2001; accepted for publication 31 May 2001.

*Associate Professor, School of Aerospace and Mechanical Engineering.
†Graduate Student, School of Aerospace and Mechanical Engineering; currently Researcher, MIRU Corporation 138-702, Republic of Korea.
‡Assistant Professor, School of Aerospace and Mechanical Engineering.
§Professor, School of Aerospace and Mechanical Engineering.
¶Associate Professor, Department of Avionics Engineering.